Development of a lung-liver in vitro coculture model for inhalation-like toxicity assessment

Sabrina Madiedo-Podvrsan, Louise Sebillet, Thomas Martinez, Salimata Bacari, Fengping Zhu, Marie Cattelin, Eric Leclerc, Franck Merlier, Rachid Jellali, Ghislaine Lacroix, et al.

Development of a lung-liver *in vitro* coculture model for inhalation-like toxicity assessment

Sabrina Madiedo-Podvrsan[1], Louise Sebillet[1], Thomas Martinez[2], Salimata Bacari[1], Fengping Zhu[1], Marie Cattelin[1], Eric Leclerc[3], Franck Merlier[4], Rachid Jellali[1], Ghislaine Lacroix[2], Muriel Vayssade[1*]

[1] Université de technologie de Compiègne, CNRS, Biomechanics and Bioengineering, Centre de recherche Royallieu - CS 60319 - 60203 Compiègne Cedex, France

[2] French National Institute for Industrial Environment and Risks, INERIS, Direction milieux et impacts sur le vivant, Verneuil-en-Halatte, France

[3] CNRS IRL 2820, Laboratory for Integrated Micro Mechatronic Systems, Institute of Industrial Science, University of Tokyo, 4-6-1 Komaba, Meguro-ku, Tokyo, Japan

[4] Université de technologie de Compiègne, UPJV, CNRS Enzyme and Cell Engineering Laboratory, Centre de recherche Royallieu - CS 60319 – 60203 Compiègne Cedex, France

* Correspondence: muriel.vayssade@utc.fr ; Phone: +33 3 44 23 73 09

Abstract

Animal models are considered prime study models for inhalation-like toxicity assessment. However, in light of animal experimentation reduction (3Rs), we developed and investigated an alternative *in vitro* method to study systemic-like responses to inhalation-like exposures. A coculture platform was established to emulate inter-organ crosstalks between a pulmonary barrier, which constitutes the route of entry of inhaled compounds, and the liver, which plays a major role in xenobiotic metabolism. Both compartments (Calu-3 insert and HepG2/C3A biochip) were jointly cultured in a dynamically-stimulated environment for 72 hours. The present model was characterized using acetaminophen (APAP), a well-documented hepatotoxicant, to visibly assess the passage and circulation of a xenobiotic through the device. Based on viability and functionality parameters the coculture model showed that the bronchial barrier and the liver biochip can successfully be maintained viable and function in a dynamic coculture setting for 3 days. In a stress-induced environment, present results reported that the coculture model emulated active and functional *in vitro* crosstalk that seemingly was responsive to xenobiotic exposure doses. The hepatic and bronchial cellular responses to xenobiotic exposure were modified in the coculture setting as they displayed earlier and stronger detoxification processes, highlighting active and functional organ crosstalk between both compartments.

Keywords: bioengineering, multiorgan-on-a-chip, toxicology, coculture, lung-liver crosstalk

Graphical abstract

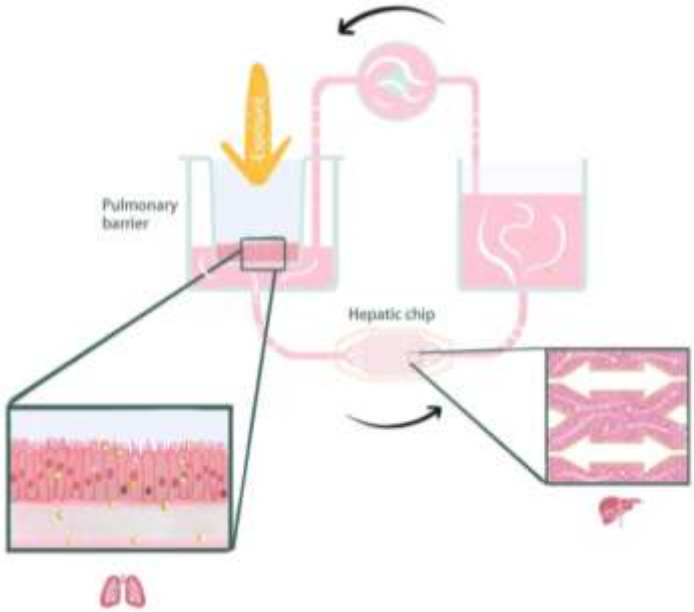

Highlights:

1. A bronchial barrier and a liver biochip were successfully maintained viable and functional in a dynamic coculture setting.
2. The coculture model is responsive to xenobiotic exposures and emulates active and functional *in vitro* crosstalk between both tissue constructs.
3. The lung-liver crosstalk induces a modulation of stress response kinetics, delaying cytotoxicity.

1. Introduction

Modern urbanization and globalization phenomena multiply and complexify pollution sources. Among them, air pollution has an increasingly significant impact on global health due to its transboundary nature (Cohen et al., 2017; O'Neill et al., 2011; Solomon et al., 2011). A recently published review reports that air pollution causes over 6.5 million deaths each year globally, and that this number is increasing (Fuller et al., 2022). Air quality is closely linked to anthropogenic pollution sources mainly defined by industrial processes, domestic pollution, transportation and agricultural systems.

The lungs are the main route of entry of airborne xenobiotics. Upon internalization, inhaled compounds undergo absorption, distribution, metabolism, and excretion (ADME) processes which lead them to interact with pulmonary and extra-pulmonary cells (Castell et al., 2005). Associated toxicity mechanisms are complex and involve local and systemic responses that can aggravate, stabilize, or protect the body from adverse effects. Because of this complexity, animals are considered prime study models. However, in the European context of animal experimentation reduction (3Rs) the development of reliable alternative methods has become a necessity. *In vitro* models are particularly interesting because they are cost-effective and easier to implement than *vivo* models. However, since tissues and organs reside *in vivo* in highly integrated and dynamically interactive environments, extrapolation from *vitro* to *vivo* is limited if inter-organ crosstalk is not considered. Multi-organ-on-a-chip technologies seek to overcome these limitations by connecting multiple metabolically active organoids within a single culture circuit to mimic systemic-like interactions. The literature reports numerous cases of multi-organ platforms comprising a pulmonary compartment (Hübner et al., 2018; Kimura et al., 2015; Skardal et al., 2017), however only a minority considers and studies the lungs as a key route of entry in the ADME process.

Since hepatic xenobiotic metabolism is strongly tied to systemic toxicity *in vivo*, and the literature reports instances of lung-liver crosstalk in stress-induced environments, investigation of hepatic responses to respiratory stress was given consideration (Guo et al., 2019; Kim et al., 2014; Ya et al., 2018). Here, we describe a coculture model designed to investigate inhalation-like toxicity in a further systemic manner by connecting *in vitro*, through microfluidics, a pulmonary barrier to a detoxifying organ such as the liver. Our approach considers the lungs as a route of entry and intends to study the metabolic fate of inhaled compounds by considering inter-organ crosstalk as possible modulators of toxicity. Even though a few other lung-liver coculture systems have previously been described (Bovard et al., 2018; Coppeta et al., 2017; Schimek et al., 2020), the metabolic fate of xenobiotics has not been studied.

The present lung-liver model was characterized using a well-documented hepatotoxicant: acetaminophen also known as paracetamol (APAP). The coculture was exposed to APAP through the pulmonary barrier, to imitate an inhalation type exposure. APAP exposure allows us to visibly assess the passage and circulation of a model substance through the device, as it interferes with hepatic viability and metabolic performances.

2. Material & Methods

2.1. Calu-3 tissue culture

Cryopreserved Calu-3 (ATCC, reference HTB-55) cells were grown and expanded using Roswell Park Memorial Institute 1640 supplemented with stable L-Glutamine (RPMI 1640 GlutaMAX Supplement, ThermoFischer Scientific), and completed with 10% of Fetal Bovine Serum (FBS, Gibco) and 1% of 100 units/mL Penicillin-Streptomycin (PAN Biotech). Cells were amplified in 75 cm^2 flasks (Corning, Falcon) seeded at an initial density of 20 000 cells per cm^2, in a 37°C, 5% CO_2 incubator. Once cells reached 80% of confluence, they were

detached using trypsin-EDTA (1X) (Gibco) and seeded, at 200.10^3 cells per 6-plate sized Transwell culture insert. Tissues were grown under static submerged conditions, i.e. tissues were apically covered by culture media, for 11 days when trans-epithelial resistance (TEER) measurements exceeded 1000 $\Omega.cm^2$ (Figure 1A). As soon as the bronchial barrier completes reconstruction, Calu-3 inserts were transferred in the coculture platform and submerged tissues underwent 72-hour of perfused culture at a continuous microfluidic flow rate of 25 µL per min (Figure 1B and C). Medium perfusion was perceived on the basolateral side of the culture insert. Calu-3 tissue culture was carried out for a total of 14 days.

2.2. HepG2/C3A biochip cultures

2.2.1. Biochip design and microfabrication. The design and fabrication of the biochip has been previously documented (Baudoin et al., 2011). Briefly, the inner microarchitecture of biochips is printed by photolithography onto wafer containing SU-8 photoresist. The design comprises two sides, a hollow media reservoir for the upper compartment and a series of microstructured chambers and channels for the bottom cell cultivating side. 10:1 (w/w) polydimethylsiloxane (PDMS) and cross-linking agent (Sylgard 184, Dow Corning) mixture was used to manufacture biochips. The mix was poured onto the microdesigned molds and cured for 2 hours at 70°C. Reactive air plasma treatment of surfaces allowed to seal both sides together to achieve the completed biochip. The final assembled biochip holds a total volume of 40 µL and covers a cell growth area of $2cm^2$. Prior to cell culture, biochips are sterilized by autoclave, and coated with a 0.36 mg/ml Collagen I (Corning Life Science) solution to allow cell adhesion.

2.2.2. Biochip hepatic cell culture. Hepatocellular carcinoma-derived HepG2/C3A cells (ATCC, reference CRL-10741) were grown and expanded using Minimum Essential Medium (MEM, Corning) supplemented with 10% FBS, 1% of Penicillin-Streptomycin, 1% of L-

Glutamine (100X) (PAN Biotech), 1% of N-2-hydroxyethylpiperazine-N-2-ethane sulfonic acid (HEPES) buffer (1M) (Gibco), 1% of Sodium Pyruvate (100X) (Gibco) and 1% of MEM non-essential amino acids (BioWest). Cells were amplified in 75 cm^2 flasks (Corning, Falcon), seeded at an initial density of 20 000 cells per cm^2, in a 37°C, 5% CO_2 incubator. Once cells reached 90% of confluence, they were detached using trypsin-EDTA (Gibco) and seeded, into culture ready-biochips at an initial density of 500.10^3 cells per biochip. Seeded biochips were kept at rest 24 hours, in a 37°C, 5% CO_2 incubator, to complete cell adhesion. Biochips were then boxed into an Integrated Dynamic Cell Culture in Microsystems (IDCCM) device (Patent - {US20130084632A1}), perfused culture was maintained for 72 hours at a continuous microfluidic flow rate of 25 µL per min thanks to a peristaltic pump.

2.3. Coculture

2.3.1 Coculture box: Integrated Insert in a Dynamic Microfluidic Platform (IIDMP). Both compartments were serially connected using the Integrated Insert in Dynamic Microfluidic Platform (IIDMP) device (Bricks et al., 2014). This coculture platform is a polycarbonate-based box able to accommodate 3 parallelized cocultures (Figure 1D and E). The bottom side comprises wells for 6-plate sized Transwell culture inserts, attachments for biochips and associated media reservoirs, and a top lid for tubing. Both parts are joined and sealed together by a silicon seal and screws. Once mounted, the device is set at a continuous microfluidic flow rate of 25 µL per min, thanks to a peristaltic pump. Flow was directed from the insert to the biochip in a closed loop.

2.3.2. Bronchial and hepatic coculture conditions. Calu-3 inserts and HepG2/C3A biochips were matured separately, according to previously described protocols, before being joined in culture for 72 hours in RPMI-based medium, in a 37°C, 5% CO_2 incubator.

Acetaminophen (APAP, Sigma Aldrich) was dissolved in RPMI-based medium and APAP solutions (1 mL) were deposited apically on the pulmonary barrier at local exposure concentrations of 7.5 and 15 mM, which dilute into the circulating media respectively to systemic concentrations of 1.5 and 3 mM when exposure solution joins the dynamic circulation within the device.

2.4. Cell proliferation assays

2.4.1. Mitochondrial activity assessment. Calu-3 mitochondrial activity was assessed by Prestoblue assay (Prestoblue^{TM} Cell viability Reagent, Fischer Scientific). Non-cytotoxic fluorogenic probe passively entered living cells in its non-fluorescent form (reazurin) and reduced into resorufin by mitochondria, a soluble red fluorescent product, that diffused out of the cells and was directly measured by spectrophotometry (excitation wavelength of 535 nm and emission wavelength of 595 nm, Spectafluor Plus, TECAN).

2.4.2. Cell count. HepG2/C3A cells within post-culture biochips were detached using trypsin-EDTA and counted using a Malassez' hemocytometer. Cell viability was assessed by Trypan blue dye exclusion.

2.5. Calu-3 tissue barrier properties

2.5.1. Trans-epithelial electrical resistance measurement. The quantitative measurement of barrier integrity was achieved using double electrodes (STX2 set and EndOhm-24SNAP 147581 from World Precision Instruments) connected to Millicell-ERS (Electrical Resistance System) (Millipore) to measure passing current. Every series of measurements included measuring the blank resistance (R_{BLANK}) of an acellularized membrane and the resistance across a cellularized membrane (R_{TOTAL}). TEER values are reported ($TEER_{REPORTED}$) in units of $\Omega.cm^2$ and calculated as:

$$TEER_{REPORTED} = (R_{TOTAL} - R_{BLANK})(\Omega) \times M_{AREA}(cm^2)$$

2.5.2. Adherens and tight junction immunostaining. Post-culture exposed and non-exposed samples were collected, rinsed 3 times with PBS (1X, pH 7.4, Gibco) and fixed with 4% paraformaldehyde (PFA) solution. Cells were permeabilized with 100X Triton (BDH) à 0.1% at room temperature. Non-specific sites were blocked by immersing the sections into 2% bovine serum albumin (BSA, Gibco). Primary antibodies (rat anti-CD324 antibody, Invitrogen 5µg/mL or rabbit anti-Claudin 1 antibody MH25, Invitrogen 20 µg/mL) were added to the sections for 1 hour at room temperature. Then, the sections were rinsed 3 times with PBS at room temperature. Secondary antibodies (Cyanine 2 AffiniPure goat anti-rat IgG secondary antibody, 1:100, Jackson ImmunoResearch or AlexaFluor 680 goat anti-rabbit IgG secondary antibody, 4 µg/mL, Thermo Scientific), were added to the sections for 1 hour at room temperature in a dark chamber. The samples were rinsed 3 last times with PBS at room temperature and received a 1 mg/mL 4′,6-diamidino-2-phenylindole (DAPI) immunostaining (MBD0015, Merck) for nuclei staining. Immunofluorescence microscopy scans where achieved with confocal microscopy (Zeiss LSM 710).

2.5.3. MUC5AC dosage. Quantitative detection of MUC5AC in post-culture supernatant samples was achieved using the Human MUC5AC ELISA kit (CliniSciences) according to manufacturer instructions.

2.5.4. Lucifer Yellow permeability assay. Barrier function was quantified by Lucifer Yellow permeability assay (LY) (Lucifer Yellow CH dipotassium salt, Sigma-Aldrich) on post-culture Calu-3 tissues. Briefly, tissues were washed with pre-warmed (37°C) HBSS (with $CaCl_2$ and $MgCl_2$, pH 7.4, Invitrogen) on both apical and baso-lateral compartments. Lucifer Yellow CH dipotassium salt was then diluted in HBSS and added to the donor compartment at a final concentration of 100 µg/mL. After 1 hour of incubation at 37°C and 5% CO_2, aliquots from the donor and receiver compartments were collected in a black 96-well micro-

plate for determination of fluorescence leakage of the LY with a fluorescence microplate reader (TECAN, 71 Spectrafluor plus) ($\lambda_{excitation}$ = 485 nm, $\lambda_{emission}$ = 530 nm). The apparent permeability coefficient (Papp, unit: cm.s^{-1}) was calculated as follows:

$$Papp = \frac{dQ}{dt} \times \frac{1}{AC_0}$$

Where dQ/dt was the amount of compound transported per second (mg.s^{-1}), A was the surface area of the culture membrane (cm^2) and C_0 the initial donor concentration (mg/mL). The mass balance (R, unit: %) was calculated as:

$$R = 100 \times \frac{A + D}{D_0}$$

Where A and D were the amounts of compounds in the apical and basal compartments respectively, and D_0 the initial amount of Lucifer Yellow introduced at t0 in the donor compartment. Mass balances of all compounds were between 46 and 86%.

2.6. Hepatic functionality assays

2.6.1. Albumin synthesis. Hepatic albumin secretion was quantified in post-culture media samples by ELISA assay according to manufacturer instructions (Human albumin ELISA Quantitation Set, Bethyl Laboratories).

2.6.2. EROD assay (CYPA1/2 and CYP2B detoxifying activity). CYP1A1/2 and CYP2B activity levels of post-culture hepatic biochips were measured using 5-ethoxyresorufin (10 mM) as substrate. Resorufin formation by 7-ethoxyresorufin O-deethylation (EROD) was quantified by fluorescence intensity measurement ($\lambda_{excitation}$ = 535 nm, $\lambda_{emission}$ = 595 nm) (TECAN, Spectrafluor plus) after 1 h incubation in presence of salicylamide (3 mM), which inhibits phase II enzymes.

2.7. Mass spectrometry detection

An Agilent QQQ 6460 mass spectrometer with a jet stream electrospray ion source and an Agilent 1200 series fast resolution LC system (Wilmington, DE) was employed to detect acetaminophen and associated metabolites in culture medium samples. MassHunter software was used for system control, data acquisition, and data processing. LC separation was performed on an Agilent poroshel C18 reverse phase column (100 mm x 4.6 mm i.d., 2.6 μm particle size) with a gradient program at a flow rate of 1 mL/min. The mobile phase A consisted of 100% HPLC grade water with 0.1% formic acid and mobile phase B consisted of 100% HPLC grade acetonitrile. The gradient started with 2% solvent B, held at 2% B for 1 minute before being increased to 20% B then increased to 95% in 1 minute and was then held at 95% B for 2 additional minutes. The column was re-equilibrated with 2% B for 3 minutes. Total run time was 12 minutes with a 10 μL injection volume. The mass spectrometer was operated in positive and negative jet stream ESI modes. Nitrogen was used as a nebulizer, turbo (heater) gas, curtain, and collision-activated dissociation gas. The capillary voltage was +3800 V and -3500 V. The ion source gas temperatures were 350°C with flows of 12 L/min. Jetstream gas temperatures were 350°C with flows of 12 L/min. APAP and metabolites were measured by selective reaction monitoring (SRM). The calibration curve was performed with internal calibration using 0.5 μM APAP-D4 in acetonitrile. The samples are prepared by taking 20 μL of medium and adding 80 μL of the internal standard solution to the acetonitrile in a 1 mL glass vial, then centrifuged for 5 minutes at 13500 rpm before being transferred from a vial with a 200 μL glass insert.

2.8. Statistical analysis

Data are presented as the mean ± standard deviations. Histogram charts are complemented by scatter plots, which gather the samples that constitute the groups. n represents the number of independent experiments performed. Group comparison statistical tests were chosen based on

analysis of dataset variance and normality. All data was unpaired. Two-group comparisons were carried out by unpaired t-test, and Mann-Whitney test respectively for normal and non-normal data. Multiple group comparisons were carried out by ANOVA, and Kruskal-Wallis test respectively for normal and non-normal data. Statistical analysis was performed using GraphPad Instat v.3.10. P values less than 0.05 were considered statistically significant and are presented as follow: *$p<0.05$, **$p<0.01$, ***$p<0.001$.

3. Results

3.1. Characterization of Calu-3 behavior to coculture

For bronchial tissues to acquire proper barrier function, through the development of solid junctional networks, Calu-3 cells were cultured for 11 days until trans-epithelial resistance (TEER) measurements exceed 1000 $\Omega.cm^2$. Mature constructs on inserts were then cultured in a dynamically-stimulated environment for 72h, in monoculture or coculture (with liver biochip) settings. To ensure accurate readout, viability and functionality parameters of cocultured tissues were monitored post-culture and results were compared to monoculture data.

A global overview of tissue integrity was assessed through phase-contrast microscopy observations (Figure 2A). Overall, coculture did not seem to disturb the morphological development of Calu-3 bronchial tissues: no difference in cell refringence was noted between monoculture and coculture. The culture mode did not visually perturb adhesion and proliferation trends of Calu-3 cells as both tissues remained homogenous and displayed similar confluence and cohesiveness.

Calu-3 tissues also seemed to seamlessly adapt to the coculture environment as mitochondrial activity data showed that the presence of the hepatic compartment had no significant impact on cell metabolic activity compared to that of monocultured cells (Figure 2B). From a

functional standpoint, Calu-3 tissues formed and maintained strong barrier integrity (Figure 2C), as non-invasive TEER measurements revealed that values stabilized at 2500 $\Omega.cm^2$, and continued to apically release gel-forming mucins MUC5AC (Figure 2D) regardless of culture conditions.

Intercellular junction immunostainings allowed to further depict the barrier integrity status of cocultured tissues (Figure 3). The staining of E-Cadherin remained localized at the cell-cell interface without any diffusion, whereas Claudin-1 expression appeared disrupted from its native peripheral localization compared to monocultured samples.

Despite the alteration of the tight junction network of cocultured Calu-3 tissues, Lucifer Yellow assays revealed no significant permeability rates between tissues of different culture settings (Table 1). Overall, permeability remained minimal, under 1%, coculture did not disrupt the permeability of the barrier.

3.2. Characterization of HepG2/C3A behavior to coculture

Prior to coculture, common medium tests were conducted to ensure optimal maintenance of tissue viability and functionality of both compartments (data not shown). As HepG2/C3A cellular behavior in RPMI-based medium remained comparable to that of initial MEM-based medium (no cell death induction, stable CYP1A activity), RPMI-based medium was used for coculture purposes. Cocultured hepatic biochips were collected post-culture and underwent a variety of assays to assess the impact of coculture on hepatic functions.

Phase contrast microscopy showed that adhesion and proliferation of hepatocytes within the biochip were successful despite the culture mode, as cells were homogeneously spread throughout the microchambers and channels of the system (Figure 4A). Overall, morphological features seemed to remain unchanged, cocultured HepG2/C3A biochips continued displaying confluent and cohesive tissues.

Quantitative assessments of cell viability and functionality confirmed these qualitative observations: cocultured biochips maintained similar cell density (approximating $1.5.10^6$ cells per biochip, Figure 4B) and hepatic differentiation (HepG2/C3A albumin secretion stabilized at 200 ng/10^6 cells/h, Figure 4C). In terms of hepatic xenobiotic response, the results showed that coculture induced an induction of CYP1A1/2 activity as rates nearly doubled compared to their monocultured counterparts (Figure 4D).

3.3. Stability and response of the lung/liver coculture to a stress-induced environment

Following the characterization of the suitability of both pulmonary and hepatic *in vitro* building blocks in a joint culture setting, the lung/liver model was characterized in a stress-induced environment using APAP. The chosen exposure concentrations relied on documented hepatotoxicity thresholds, 1.5 mM and 3 mM, to allow better quantification of biological responses. First we confirmed that the culture equipment (IIDMP coculture box, culture insert, biochip, tubing) did not induce possible biases by passively absorbing a part of the exposed APAP during the culture period. APAP was introduced in the coculture system but in an acellular environment and APAP concentrations were measured after 72 hours of dynamic culture (Supplementary data, Table A). Data indicated that initial APAP concentrations were found at the same levels after 72h.

Tissue-specific APAP-induced responses were compared to coculture data to highlight crosstalk-specific responses to xenobiotic stress. Following the 72-hour coculture period, media samples were collected from the apical and baso-lateral sides of the pulmonary barrier respectively corresponding to the inhalation-like APAP exposure site, and to the circulating common culture medium. To verify that APAP was able to cross the bronchial barrier and reach the systemic circulation, APAP levels were quantified through mass spectrometry (Table 2). Results revealed that the passage into the circulating medium was successful as

APAP was detected on the apical and basal sides of the pulmonary barrier. In addition to APAP levels, secondary non-toxic metabolites (APAP-glucuronide and APAP-sulfate) were detected mainly in the basal compartments but in a non-dose dependent manner. This suggests that the lung/liver coculture was capable of metabolizing APAP at hepatotoxic exposure concentrations.

Calu-3 tissues were subject to Prestoblue assays, to determine the effect of APAP on metabolic activity (Figure 5A). APAP exposure induced a significant decrease of mitochondrial activity in Calu-3 tissues, with no dose-dependent effect. The intensity of APAP adverse effects was reduced in cocultured Calu-3 tissues: the mitochondrial activity became significant only at 3 mM and measured values were significantly higher to those obtained in monocultures.

Hepatic cell count data (Figure 5B) revealed similar response patterns, where the adverse effects induced by APAP in monoculture settings diminished in coculture. Statistical analysis revealed alleviated differences between APAP-exposed cell counts as cocultured exposed biochips featured smaller cell count variations.

Upon contact with APAP, the hepatic responses to stress differed according to culture conditions: cocultured HepG2/C3A biochips were subject to an earlier induction of CYP1A1/2 activity at 1.5 mM and decreased at 3 mM APAP exposure concentration whereas the stimulation of the activity in monocultured cells only occurs at 3 mM (Figure 5C). Moreover, at the same exposure dose (1.5 mM), the cocultured cells respond significantly stronger. The maximum intensity of CYP activity perceived under coculture conditions was about 5 times greater than that under monoculture. Maximum CYP activity peaked at 256 ± 101 pmol of resorufin per hour per 10^6 cells, whilst in monoculture the maximum only reached 75 ± 21 pmol of resorufin per hour per 10^6 cells. Thus, the metabolic profile of

HepG2/C3A biochips was impacted by the presence of a bronchial barrier in a stress-induced environment.

4. Discussion

Overall, present results show that the submerged Calu-3 bronchial barrier and the HepG2/C3A hepatic biochip can be successfully cocultured *in vitro* during 72 hours as they display stable and functional cellular behaviors. According to the collected data, the presence of a foreign tissue did not induce a stressful culture environment for either of the tissues, however, it did cause a reorganization of the Calu-3 tissue architecture. The alteration of Claudin-1 labeling at cell-cell contact sites should have resulted in increased permeability of the barrier, as they are responsible for regulating access to paracellular spaces (Anderson & Van Itallie, 1995), yet this was not the case. As the involvement of the HepG2/C3A cells in the maintenance of Calu-3 tissue permeability has not yet been observed or studied in the literature, the study of other biomarkers (such as reactive oxygen species, inflammatory cytokines …) would improve the understanding of the crosstalk between both cell types.

The quantification of APAP concentration within the acellular coculture platform confirms the previously documented data (Bricks et al., 2015) which reveals that the materials of the present culture equipment don’t absorb APAP passively and that the bioavailability of paracetamol in coculture conditions remains the same as the initial exposure. The observed experimental biological effects can therefore be related to the theoretical exposure concentrations. While APAP exposures have usually only been considered on the apical side of the bronchial barrier, it is presumed that within the coculture platform APAP and its metabolites recirculate continuously throughout the culture period, which would mean that the

bronchial compartment could suffer a continuous re-exposure through is basal cell pole. The quantification of the basal permeability of the Calu-3 barrier indicates that such an APAP re-exposure is plausible as basal tissue permeability ($0.071 \pm 0.03 \times 10^{-6}$ $cm.s^{-1}$) is similar to apical permeability ($0.049 \pm 0.01 \times 10^{-6}$ $cm.s^{-1}$).

The coculture setting allowed the passage of APAP through the Calu-3 barrier and into the circulatory system, as APAP was detected in the circulating medium and likely reached the liver compartment as the hepatic homeostasis of the biochip was impaired. Overall APAP exposures elicited similar cellular behavior patterns, associated with apparent cytotoxicity. However, the intensity of associated adverse effects was reduced, and tissue responses followed a different kinetic in the coculture setting. While the presence of APAP-glucuronide and APAP-sulfate in the medium is indicative of active phase II metabolism, CYP1A activity measurements allow following phase I oxidation metabolism. Results show that in the coculture setting, APAP induces earlier and 5-fold stronger CYP1A activities than in monoculture. CYP1A is involved in the biotransformation of APAP into reactive N-acetyl-p-benzoquinone imine (NAPQI) (Prot et al., 2011a) which is known to be the toxic metabolite of APAP (Larson, 2007; Mazaleuskaya et al., 2015). Increased CYP1A activity should be related to greater cytotoxicity, but because this was not the case, this could imply that NAPQI is actively detoxified. Possible detoxification would explain why the mitochondrial metabolism of cocultured Calu-3 is higher than in the monoculture setting, as literature reports how NAPQI targets mitochondrial proteins (Qiu et al., 1998). As the exposure concentration rises (3 mM), the lung/liver coculture seems to display disrupted xenobiotic metabolism respectively as CYP1A activity reduces and APAP-glucuronide and APAP-sulfate metabolites are absent on the apical side of the bronchial barrier. As a result, produced NAPQI could freely circulate through the coculture, no longer undergoing enhanced

detoxification processes previously described, which would explain at least partly why the adverse effects are more pronounced than for 1.5 mM-APAP exposed cocultures. Delayed cytotoxicity suggests that at least a part of the NAPQI was metabolized into a non-toxic metabolite, implying that the detoxification metabolism would have been at least momentarily active during the 72-hour culture period, before the exhaustion of cellular defense mechanisms. To verify this hypothesis, together with direct measurement of NPAQI and APAP-glutathione metabolites in the system, the state of Calu-3 and HepG2/C3A metabolisms could be punctually assessed throughout the coculture period to verify if a gradual decrease occurs. Our results coincide with Bovard et al. (2018) and Schimek et al. (2020) who also highlighted that bronchial tissue/HepaRG spheroids cocultures induced a modulation of toxicity in a stress environment upon exposure to aflatoxin B1. Because the authors did not assess the presence of metabolites in their platform, they could not conclude with certainty that the xenobiotic was metabolized: this is not the case in the lung-liver coculture model we describe, which is metabolically competent (assessed with CYP1A activity induction and APAP-glucuronide and APAP-sulfate metabolites detection).

The biochip employed in the coculture has been previously developed, characterized and optimized for hepatic tissue culture. This microsystem was utilized for short- and long-term cultures of cell lines but also primary (rat and human hepatocytes) and stem cells (Essaouiba et al., 2022; Prot et al., 2011a, 2011b; Legendre et al., 2013; Jellali et al., 2016; Danoy et al., 2021; Etxeberria et al., 2022). It has already been used successfully for many toxicity and metabolic studies (Baudoin et al., 2013; Jellali et al., 2018, 2021; Prot et al., 2011b), and numerous coculture models (Bricks et al., 2015; Danoy et al., 2021; Essaouiba et al., 2020; Prot et al., 2014; Zeller et al., 2017). Recently, hydrogel and hydroscaffolds were integrated in the biochip to promote liver cell organization in 3D spheroids/organoids (Boulais et al., 2020; Messelmani et al., 2022). Regarding the pulmonary barrier, in addition to simplistic model

presented here, our team developed multicellular alveolo-capillary barrier including macrophages and pulmonary endothelial cells (Dekali et al., 2014). Along with the potential that the liver biochip and lung barrier models offers, air-liquid aerosolized exposure could offer promising complexification opportunities to the present coculture model and therefore empower its relevance for the risk assessment of inhaled xenobiotics. Indeed the IIDMP platform is equipped with inlet port (top of insert compartment) allowing the connection to aerosol generator such as Vitrocell® system (Loret et al., 2018). Furthermore, the use of human primary cells and chronic exposures to well-known inhaled compounds would be needed to expand the significance of the current model.

5. Conclusions

Our data indicate that a Calu-3 bronchial barrier and a HepG2/C3A biochip can be successfully maintained viable and functional in a dynamic coculture setting for 3 days. The developed model is seemingly responsive to xenobiotic exposures, and emulates active and functional *in vitro* crosstalk between both compartments, allowing to obtain preliminary investigative predictions in 72 hours. The crosstalk induced a modulation of stress response kinetics, delaying cytotoxicity, proving that xenobiotic fate and biological behaviors can be modulated in a broader systemic-like environment. The present lung/liver coculture displays promising potential to empower the prediction of inhalation-like exposures.

6. Acknowledgments

The work was funded by the European Regional Development Fund (ERDF) 2014/2020 and the national research program Environnement-Santé-Travail (PNR EST) of the French National Food Safety Agency (Anses).

The graphical abstract was designed and realized by Dr Augustin Lerebours.

7. Bibliography

- Anderson, J. M., Van Itallie, C. M. (1995). Tight junctions and the molecular basis for regulation of paracellular permeability. Am. J. Physiol. 269, G467-475. https://doi.org/10.1152/ajpgi.1995.269.4.G467

- Baudoin, R., Griscom, L., Prot, J. M., Legallais, C., Leclerc, E. (2011). Behavior of HepG2/C3A cell cultures in a microfluidic bioreactor. Biochem. Eng. J. 53, 172–181. https://doi.org/10.1016/j.bej.2010.10.007

- Baudoin, R., Prot, J. M., Nicolas, G., Brocheton, J., Brochot, C., Legallais, C., Benech, H., Leclerc, E. (2013). Evaluation of seven drug metabolisms and clearances by cryopreserved human primary hepatocytes cultivated in microfluidic biochips. Xenobiotica. 43, 140–152. https://doi.org/10.3109/00498254.2012.706725

- Boulais, L., Jellali, R., Pereira, U., Leclerc, E., Bencherif, S. A., Legallais, C. (2021). Cryogel-Integrated Biochip for Liver Tissue Engineering. ACS Appl. Bio. Mater. 4, 5617–5626. https://doi.org/10.1021/acsabm.1c00425

- Bovard, D., Sandoz, A., Luettich, K., Frentzel, S., Iskandar, A., Marescotti, D., Trivedi, K., Guedj, E., Dutertre, Q., Peitsch, M. C., Hoeng, J. (2018). A lung/liver-on-a-chip platform for acute and chronic toxicity studies. Lab Chip. 18, 3814–3829. https://doi.org/10.1039/C8LC01029C

- Bricks, T., Hamon, J., Fleury, M. J., Jellali, R., Merlier, F., Herpe, Y. E., Seyer, A., Regimbeau, J. M., Bois, F., Leclerc, E. (2015). Investigation of omeprazole and phenacetin first-pass metabolism in humans using a microscale bioreactor and pharmacokinetic models. Biopharm. Drug Dispos. 36, 275–293. https://doi.org/10.1002/bdd.1940

- Bricks, T., Paullier, P., Legendre, A., Fleury, M.J., Zeller, P., Merlier, F., Anton, P.M., Leclerc, E. (2014). Development of a new microfluidic platform integrating co-cultures of intestinal and liver cell lines. Toxicol. In Vitro. doi: 10.1016/j.tiv.2014.02.005

- Castell, J. V., Teresa Donato, M., & Gómez-Lechón, M. J. (2005). Metabolism and bioactivation of toxicants in the lung. The in vitro cellular approach. Exp. Toxicol. Pathol. 57, 189–204. https://doi.org/10.1016/j.etp.2005.05.008

- Cohen, A. J., Brauer, M., Burnett, R., Anderson, H. R., Frostad, J., Estep, K., Balakrishnan, K., Brunekreef, B., Dandona, L., Dandona, R., Feigin, V., Freedman, G., Hubbell, B., Jobling, A., Kan, H., Knibbs, L., Liu, Y., Martin, R., Morawska, L., … Forouzanfar, M. H. (2017). Estimates and 25-year trends of the global burden of disease attributable to ambient air pollution: An analysis of data from the Global Burden of Diseases Study 2015. Lancet. 389, 1907–1918. https://doi.org/10.1016/S0140-6736(17)30505-6

- Coppeta, J. R., Mescher, M. J., Isenberg, B. C., Spencer, A. J., Kim, E. S., Lever, A. R., Mulhern, T. J., Prantil-Baun, R., Comolli, J. C., Borenstein, J. T. (2017). A portable and reconfigurable multi-organ platform for drug development with onboard microfluidic flow control. Lab Chip. 17, 134–144. https://doi.org/10.1039/C6LC01236A

- Danoy, M., Tauran, Y., Poulain, S., Jellali, R., Bruce, J., Leduc, M., Le Gall, M., Koui, Y., Arakawa, H., Gilard, F., Gakiere, B., Kato, Y., Plessy, C., Kido, T., Miyajima, A., Sakai, Y., Leclerc, E. (2021). Investigation of the hepatic development in the coculture of hiPSCs-derived LSECs and HLCs in a fluidic microenvironment. APL Bioeng. 5, 026104. https://doi.org/10.1063/5.0041227

- Dekali, S., Gamez, C., Kortulewski, T., Blazy, K., Rat, P., Lacroix, G. (2014). Assessment of an in vitro model of pulmonary barrier to study the translocation of nanoparticles. Toxicol. Rep. 1, 157–171. https://doi.org/10.1016/j.toxrep.2014.03.003

- Essaouiba, A., Okitsu, T., Kinoshita, R., Jellali, R., Shinohara, M., Danoy, M., Legallais, C., Sakai, Y., Leclerc, E. (2020). Development of a pancreas-liver organ-on-chip coculture model for organ-to-organ interaction studies. Biochem. Eng. J. 164, 107783. https://doi.org/10.1016/j.bej.2020.107783

- Etxeberria, L., Messelmani, T., Badiola, J.H., Llobera, A., Fernandez, L., Vilas-Vilela, J.L., Leclerc, E., Legallais, C., Jellali, R., Zaldua, A.M. (2022). Validation of HepG2/C3A Cell Cultures in Cyclic Olefin Copolymer Based Microfluidic Bioreactors. Polymers. 14, 4478. https://doi.org/10.3390/polym14214478

- Fuller, R., Landrigan, P. J., Balakrishnan, K., Bathan, G., Bose-O'Reilly, S., Brauer, M., Caravanos, J., Chiles, T., Cohen, A., Corra, L., Cropper, M., Ferraro, G., Hanna, J., Hanrahan, D., Hu, H., Hunter, D., Janata, G., Kupka, R., Lanphear, B., … Yan, C. (2022). Pollution and health: A progress update. Lancet Planet. Health. 6, e535–e547. https://doi.org/10.1016/S2542-5196(22)00090-0

- Guo, Y., Xiao, D., Yang, X., Zheng, J., Hu, S., Wu, P., Li, X., Kou, H., Wang, H. (2019). Prenatal exposure to pyrrolizidine alkaloids induced hepatotoxicity and pulmonary injury in fetal rats. Reprod. Toxicol. 85, 34–41. https://doi.org/10.1016/J.REPROTOX.2019.02.006

- Hübner, J., Raschke, M., Rütschle, I., Gräßle, S., Hasenberg, T., Schirrmann, K., Lorenz, A., Schnurre, S., Lauster, R., Maschmeyer, I., Steger-Hartmann, T., Marx, U. (2018). Simultaneous evaluation of anti-EGFR-induced tumour and adverse skin effects in a microfluidic human 3D co-culture model. Sci. Rep. 8, Article 1. https://doi.org/10.1038/s41598-018-33462-3

- Jellali, R., Bricks, T., Jacques, S., Fleury, M. J., Paullier, P., Merlier, F., Leclerc, E. (2016). Long-term human primary hepatocyte cultures in a microfluidic liver biochip show maintenance of mRNA levels and higher drug metabolism compared with Petri cultures. Biopharm. Drug Dispos. 37, 264–275. https://doi.org/10.1002/bdd.2010

- Jellali, R., Jacques, S., Essaouiba, A., Gilard, F., Letourneur, F., Gakière, B., Legallais, C., Leclerc, E. (2021). Investigation of steatosis profiles induced by pesticides using liver organ-on-chip model and omics analysis. Food Chem. Toxicol. 152, 112155. https://doi.org/10.1016/j.fct.2021.112155

- Jellali, R., Zeller, P., Gilard, F., Legendre, A., Fleury, M. J., Jacques, S., Tcherkez, G., & Leclerc, E. (2018). Effects of DDT and permethrin on rat hepatocytes cultivated in microfluidic biochips: Metabolomics and gene expression study. Environ Toxicol Pharmacol. 59, 1-12. https://doi.org/10.1016/j.etap.2018.02.004

- Kim, J. W., Park, S., Lim, C. W., Lee, K., Kim, B. (2014). The Role of Air Pollutants in Initiating Liver Disease. Toxicol. Res. 30, 65-70. https://doi.org/10.5487/TR.2014.30.2.065

- Kimura, H., Ikeda, T., Nakayama, H., Sakai, Y., Fujii, T. (2015). An On-Chip Small Intestine–Liver Model for Pharmacokinetic Studies. J. Lab. Autom. 20, 265–273. https://doi.org/10.1177/2211068214557812

- Larson, A. M. (2007). Acetaminophen hepatotoxicity. Clin. Liver Dis. 11, 525–548. https://doi.org/10.1016/J.CLD.2007.06.006

- Legendre, A., Baudoin, R., Alberto, G., Paullier, P., Naudot, M., Bricks, T., Brocheton, J., Jacques, S., Cotton, J., Leclerc, E. (2013). Metabolic Characterization of Primary Rat Hepatocytes Cultivated in Parallel Microfluidic Biochips. J. Pharm. Sci. 102, 3264–3276. https://doi.org/10.1002/jps.23466

- Loret, T., Rogerieux, F., Trouiller, B., Braun, A., Egles, C., Lacroix, G. (2018). Predicting the in vivo pulmonary toxicity induced by acute exposure to poorly soluble nanomaterials by using advanced in vitro methods. Part. Fibre Toxicol. 15, 25. https://doi.org/10.1186/s12989-018-0260-6

- Mazaleuskaya, L. L., Sangkuhl, K., Thorn, C. F., Fitzgerald, G. A., Altman, R. B., Klein, T. E. (2015). PharmGKB summary: Pathways of acetaminophen metabolism at the therapeutic versus toxic doses. Pharmacogenet. Genomics. 25, 416–426. https://doi.org/10.1097/FPC.0000000000000150

- Messelmani, T., Le Goff, A., Souguir, Z., Maes, V., Roudaut, M., Vandenhaute, E., Maubon, N., Legallais, C., Leclerc, E., Jellali, R. (2022). Development of Liver-on-Chip Integrating a Hydroscaffold Mimicking the Liver's Extracellular Matrix. Bioengineering. 9, 443. https://doi.org/10.3390/bioengineering9090443.

- O'Neill, M. S., Breton, C. V., Devlin, R. B., Utell, M. J. (2011). Air pollution and health: Emerging information on susceptible populations. Air Qual. Atmos. Health. 5, 189–201. https://doi.org/10.1007/S11869-011-0150-7

- Patent - {US20130084632A1} - Multi-reactor unit for dynamic cell culture. Inventor: Cécile Legallais, Régis Baudoin, Eric Leclerc, Jean-Matthieu Prot, Patrick Paullier. 2013. https://patents.google.com/patent/US10119112B2/en

- Prot, J. M., Briffaut, A.-S., Letourneur, F., Chafey, P., Merlier, F., Grandvalet, Y., Legallais, C., Leclerc, E. (2011a). Integrated proteomic and transcriptomic investigation of the acetaminophen toxicity in liver microfluidic biochip. PloS One. 6, e21268. https://doi.org/10.1371/journal.pone.0021268

- Prot, J. M., Maciel, L., Bricks, T., Merlier, F., Cotton, J., Paullier, P., Bois, F. Y., Leclerc, E. (2014). First pass intestinal and liver metabolism of paracetamol in a microfluidic platform coupled with a mathematical modeling as a means of evaluating ADME processes in humans. Biotech. Bioeng. 111, 2027–2040. https://doi.org/10.1002/bit.25232

- Prot, J.-M., Videau, O., Brochot, C., Legallais, C., Bénech, H., Leclerc, E. (2011b). A cocktail of metabolic probes demonstrates the relevance of primary human hepatocyte

cultures in a microfluidic biochip for pharmaceutical drug screening. Int. J. Pharm. 408, 67–75. https://doi.org/10.1016/j.ijpharm.2011.01.054

- Qiu, Y., Benet, L. Z., Burlingame, A. L. (1998). Identification of the hepatic protein targets of reactive metabolites of acetaminophen in vivo in mice using two-dimensional gel electrophoresis and mass spectrometry. J. Biol. Chem. 273, 17940–17953. https://doi.org/10.1074/jbc.273.28.17940

- Schimek, K., Frentzel, S., Luettich, K., Bovard, D., Rütschle, I., Boden, L., Rambo, F., Erfurth, H., Dehne, E.-M., Winter, A., Marx, U., Hoeng, J. (2020). Human multi-organ chip co-culture of bronchial lung culture and liver spheroids for substance exposure studies. Sci. Rep. 10, 7865. https://doi.org/10.1038/s41598-020-64219-6

- Skardal, A., Murphy, S. V., Devarasetty, M., Mead, I., Kang, H. W., Seol, Y. J., Zhang, Y. S., Shin, S. R., Zhao, L., Aleman, J., Hall, A. R., Shupe, T. D., Kleensang, A., Dokmeci, M. R., Jin Lee, S., Jackson, J. D., Yoo, J. J., Hartung, T., Khademhosseini, A., … Atala, A. (2017). Multi-tissue interactions in an integrated three-tissue organ-on-a-chip platform. Sci. Rep. 7, 1–16. https://doi.org/10.1038/s41598-017-08879-x

- Solomon, P. A., Costantini, M., Grahame, T. J., Gerlofs-Nijland, M. E., Cassee, F. R., Russell, A. G., Brook, J. R., Hopke, P. K., Hidy, G., Phalen, R. F., Saldiva, P., Sarnat, S. E., Balmes, J. R., Tager, I. B., Özkaynak, H., Vedal, S., Wierman, S. S. G., Costa, D. L. (2011). Air pollution and health: Bridging the gap from sources to health outcomes: Conference summary. Air Qual. Atm. Health. 5, 9–62. https://doi.org/10.1007/S11869-011-0161-4

- Ya, P., Xu, H., Ma, Y., Fang, M., Yan, X., Zhou, J., Li, F. (2018). Liver injury induced in Balb/c mice by PM 2.5 exposure and its alleviation by compound essential oils. Biomed. Pharmacother. 105, 590–598. https://doi.org/10.1016/J.BIOPHA.2018.06.010

- Zeller, P., Legendre, A., Jacques, S., Fleury, M. J., Gilard, F., Tcherkez, G., Leclerc, E. (2017). Hepatocytes cocultured with Sertoli cells in bioreactor favors Sertoli barrier tightness in rat. J. Appl Toxicol. 37, 287–295. https://doi.org/10.1002/jat.3360

Figure captions

Figure 1: Description of the lung-liver coculture model.

A: Experimental design of bronchial reconstruction; B and C: Side photos of two mounted culture-ready Integrated Insert in a Dynamic Platform (IIDMP) box on a peristaltic pump; D and E: Descriptive photos of the global structure of IIDMP box.

Figure 2: Characterization of Calu-3 tissues in mono- and cocultures.

A: Phase contrast microscopy of monocultured and cocultured Calu-3 bronchial tissues on day 14 after 72-hour dynamically-stimulated culture. Scale bar = 100 μm; B: Bronchial mitochondrial activity ($n \geq 4$, 6 samples); C: trans-epithelial electrical resistance (TEER) measurements ($n \geq 5$, 6 samples); D: MUC5AC concentrations measured by ELISA in post-culture supernatants ($n \geq 2$, 3 or 6 samples) of monocultured and cocultured Calu-3 tissues on day 14.

Figure 3: Comparison of monocultured and cocultured Calu-3 bronchial-like barriers.

Confocal microscopy imaging of nuclei (blue), E-Cadherin (red) and Claudin-1 (green) immunostained adherens and tight junction networks in monocultured and cocultured Calu-3 bronchial-like tissues on day 14. Scale bar = 20 μm.

Figure 4: Characterization of liver biochip in mono- and cocultures.

A: Phase contrast microscopy of monocultured and cocultured HepG2/C3A biochips on day 4 after 72-hour dynamically-stimulated culture. Scale bars = 250 and 100 μm; B: Evolution of HepG2/C3A cell proliferation ($n \geq 3$, at least 6 biochips); C: albumin secretion rates ($n \geq 3$, 6 biochips); D: CYP1A1/2 activities on day 4 according to culture mode ($n \geq 3$, 6 biochips).

Figure 5: Characterization of bronchial and liver tissues behavior upon exposure to APAP.

A: Bronchial mitochondrial activity of monocultured *vs* cocultured non-exposed and APAP-exposed Calu-3 tissues measured by PrestoBlueTM on day 14 after 72 hours of exposure. ($n \geq 4$, 6 samples); B: Evolution of monocultured *vs* cocultured HepG2/C3A cell proliferation according to APAP exposure concentration and culture mode ($n \geq 3$, at least 6 biochips); C: Comparison of CYP1A1/2 activities in monocultured and cocultured HepG2/C3A biochips on day 4 according to APAP exposure concentrations. ($n \geq 3$, 6 biochips).

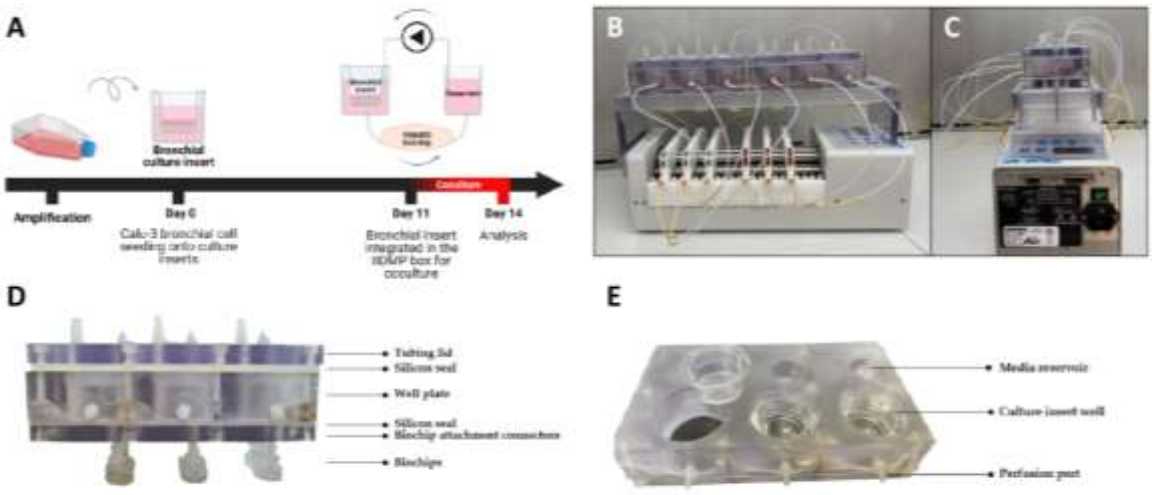
A
Bronchial culture insert
Amplification
Day 0
Day 11
Day 14
Analysis
B
C
D
E
Tubing lid
Silicon seal
Well plate
Silicon seal
Biochip attachment connectors
Biochips
Media reservoir
Culture insert well
Perfusion port

Figure 1

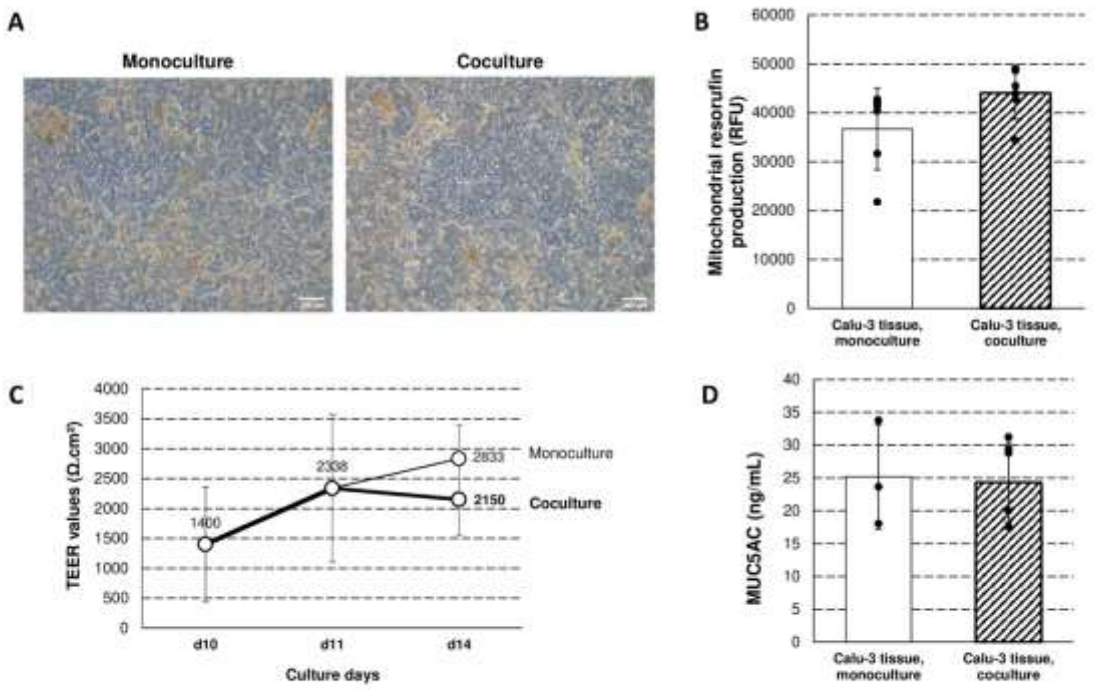
A
Monoculture
Coculture
B
Mitochondrial resorufin production (RFU)
60000
50000
40000
30000
20000
10000
0
Calu-3 tissue, monoculture
Calu-3 tissue, coculture
C
TEER values (Ω.cm²)
4000
3500
3000
2500
2000
1500
1000
500
0
1400
2398
2833
2150
Monoculture
Coculture
d10
d11
d14
Culture days
D
MUC5AC (ng/mL)
40
35
30
25
20
15
10
5
0
Calu-3 tissue, monoculture
Calu-3 tissue, coculture

Figure 2

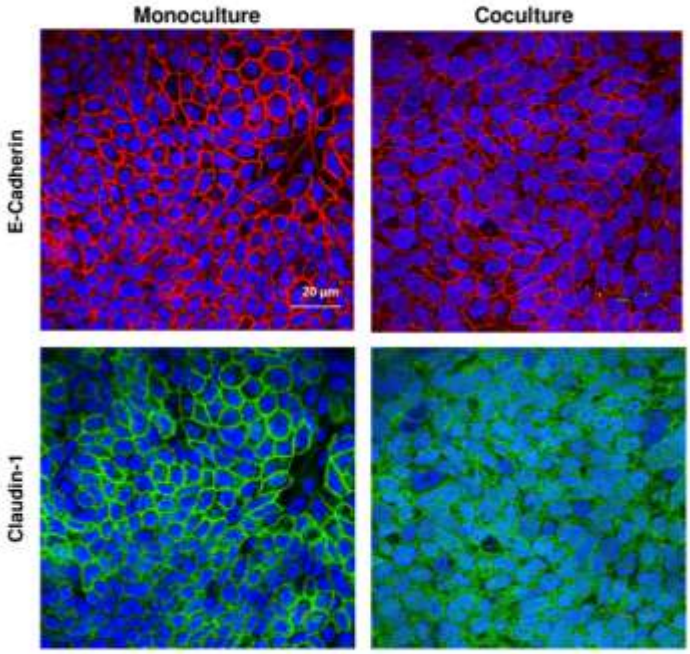

Figure 3

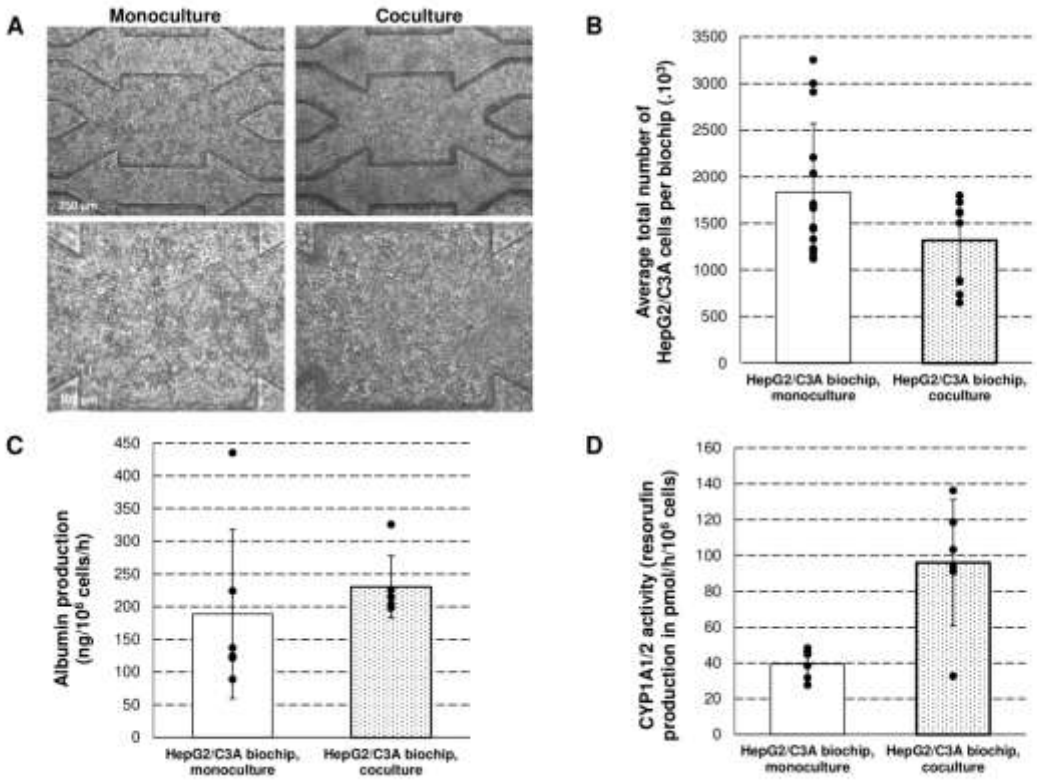
A
Monoculture
Coculture
B
Average total number of HepG2/C3A cells per biochip (.10³)
3500
3000
2500
2000
1500
1000
500
0
HepG2/C3A biochip, monoculture
HepG2/C3A biochip, coculture
C
Albumin production (ng/10⁶ cells/h)
450
400
350
300
250
200
150
100
50
0
HepG2/C3A biochip, monoculture
HepG2/C3A biochip, coculture
D
CYP1A1/2 activity (resorufin production in pmol/h/10⁶ cells)
160
140
120
100
80
60
40
20
0
HepG2/C3A biochip, monoculture
HepG2/C3A biochip, coculture

Figure 4

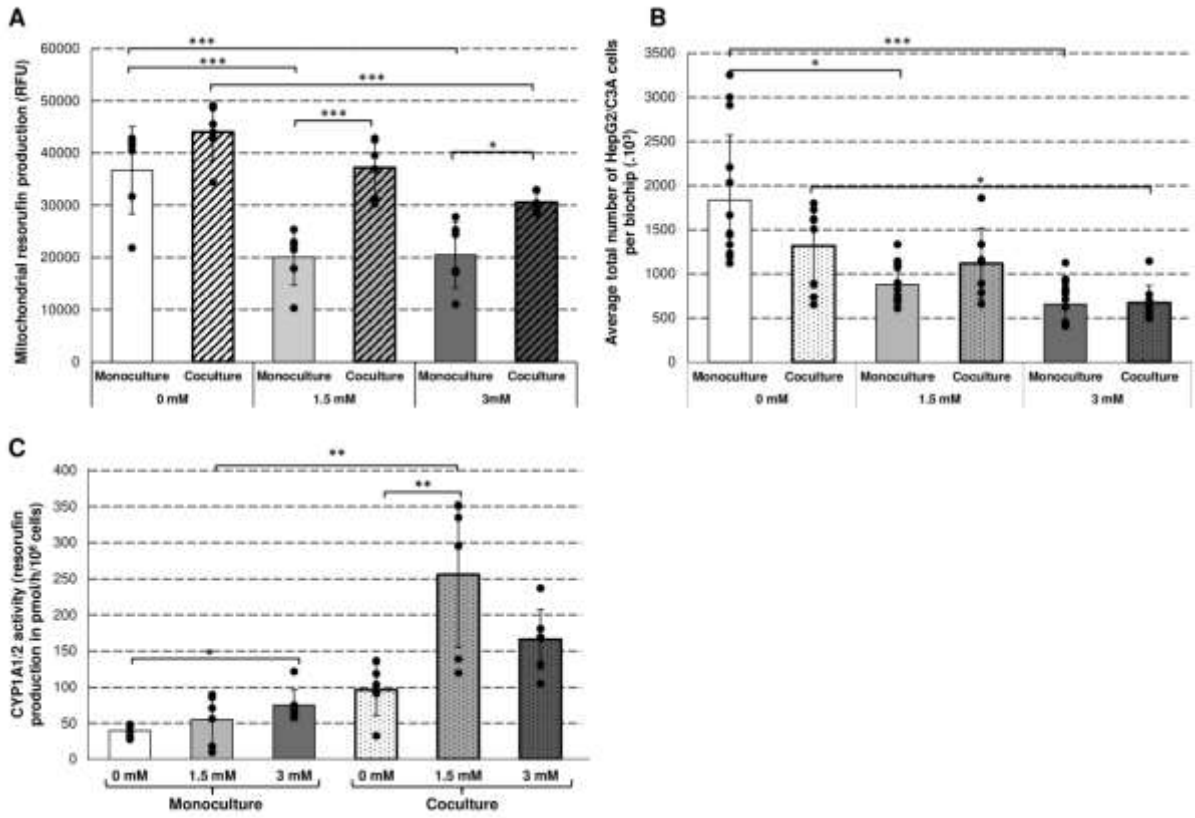
A
Mitochondrial resorufin production (RFU)
60000
50000
40000
30000
20000
10000
0
***
***
***
***
*
Monoculture
Coculture
Monoculture
Coculture
Monoculture
Coculture
0 mM
1.5 mM
3mM
B
Average total number of HepG2/C3A cells per biochip (.10³)
3500
3000
2500
2000
1500
1000
500
0
***
*
*
Monoculture
Coculture
Monoculture
Coculture
Monoculture
Coculture
0 mM
1.5 mM
3 mM
C
CYP1A1/2 activity (resorufin production in pmol/h/10⁶ cells)
400
350
300
250
200
150
100
50
0
**
**
0 mM
1.5 mM
3 mM
0 mM
1.5 mM
3 mM
Monoculture
Coculture

Figure 5

Table 1: Papp measurements of Calu-3 bronchial tissues on day 14 ($n \geq 3$, 6 samples).

	Papp ($x10^{-6}$ $cm.s^{-1}$)	Permeability rate (%)
Cell free culture insert Apical permeability	60.581	100
Monoculture	0.028 ± 0.02	0.045
Coculture	0.041 ± 0.04	0.067

Table 2: Mass spectrometry measurements of APAP and non-toxic metabolites (APAP-glucuronide and APAP-sulfate) levels in post-culture apical and basal supernatants of the lung/liver cocultures according to APAP exposure ($n \geq 3$, 6 samples).

APAP exposure (mM)		APAP (mM)	APAP-glucuronide (mM)	APAP-sulfate (mM)
Apical	0	0.013 ±0.008	0 ± 0	0 ± 0
Basal		0.005 ±0.002	0 ± 0	0 ± 0
Apical	1.5	1.844 ±0.587	0.039 ±0.092	0 ± 0
Basal		1.872 ±0.378	0.135 ±0.0140	0.012 ±0.013
Apical	3	2.267 ±1.259	0 ± 0	0 ± 0
Basal		3.178 ±0.759	0.089 ±0.122	0.007 ±0.010

Supplementary data

Table A: APAP concentrations measured with mass spectrometry after 72 hours of acellular culture in IIDMP box. N = 1.

		APAP (mM)
Apical		1.3128
Basal	1.5 mM	1.3518
Apical		2.7189
Basal	3 mM	2.6675

Declaration of interests

☒ The authors declare that they have no known competing financial interests or personal relationships that could have appeared to influence the work reported in this paper.
☐ The authors declare the following financial interests/personal relationships which may be considered as potential competing interests: